Discrete & Continuous Models
& Applied Computational Science
ISSN 2658-7149 (online), 2658-4670 (print)

2022, 30 (3) 217–230
http://journals.rudn.ru/miph

*Research article*

UDC 519.872:519.217
PACS 07.05.Tp, 02.60.Pn, 02.70.Bf
DOI: 10.22363/2658-4670-2022-30-3-217-230

# Numerical simulation of cold emission in coaxial diode with magnetic isolation

**Alexandr A. Belov[1, 2], Oleg T. Loza[2], Konstantin P. Lovetskiy[2], Sergey P. Karnilovich[2], Leonid A. Sevastianov[2]**

[1] *Lomonosov Moscow State University,*
*1, bld. 2, Leninskie Gory, Moscow, 119991, Russian Federation*
[2] *Peoples' Friendship University of Russia (RUDN University),*
*6, Miklukho-Maklaya St., Moscow, 117198, Russian Federation*

(received: July 5, 2022; revised: July 18, 2022; accepted: August 8, 2022)

**Abstract.** Due to the emergence and active development of new areas of application of powerful and super-powerful microwave vacuum devices, interest in studying the behavior of ensembles of charged particles moving in the interaction space has increased. An example is an electron beam formed in a coaxial diode with magnetic isolation. Numerical simulation of emission in such a diode is traditionally carried out using particle-in-cell methods. They are based on the simultaneous calculation of the equations of motion of particles and the Maxwell's equations for the electromagnetic field. In the present work, a new computational approach called the point macroparticle method is proposed. In it, the motion of particles is described by the equations of relativistic mechanics, and explicit expressions are written out for fields in a quasi-static approximation. Calculations of the formation of a relativistic electron beam in a coaxial diode with magnetic isolation are performed and a comparison is made with the known theoretical relations for the electron velocity in the beam and for the beam current. Excellent agreement of calculation results with theoretical formulas is obtained.

**Key words and phrases:** coaxial diode with magnetic isolation, cold emission, point macroparticles

## 1. Introduction

**Relativistic electron beams.** The existing plasma relativistic microwave generators and amplifiers (plasma masers) are based on the interaction of tubular plasma with tubular high-current relativistic electron beam (REB) [1]. The explosive-emission cathode [2] forms a tubular REB with an internal radius of ∼2 cm and a thickness of ∼0.15 cm, which propagates in a magnetic field of 1 T created by a solenoid. The electron energy in such a beam is $\sim 10^6$ eV, the electron current density is $10^3$–$10^4$ A/cm$^2$. The power of

the REB, as a rule, exceeds $10^9$ W, the current pulse lasts from several nanoseconds to several microseconds [3].

High-current relativistic electron beams are formed directly in the diode, which is supplied with a voltage pulse from the primary energy storage. Electrons receive energy only in the diode, no additional means of particle acceleration (similar to sections of linear inductive or resonant accelerators) are used. Installations for generating high-current REB are also, in some works, called direct-acting accelerators [4].

The creation of controlled beams (streams) of charged particles is carried out using a variety of devices, the main element of which is a source of charged particles. A fairly common element of such a system that provides an intense, well-focused electron beam is an electron gun. The most commonly used are thermionic guns, in which the primary element is a vacuum diode [5].

**Calculation methods.** To calculate the dynamics of electron beams, a gas-dynamic approximation is used (see, for example, [6]). As is known, the system of equations of gas dynamics is valid for thermodynamically equilibrium continuous media. Various types of equilibrium violation are taken into account using additional model assumptions. The success of this approach depends on how well the nonequilibrium model is chosen. Models that have proven themselves well in some applications (for example, nonequilibrium electronic processes of solid-state electronics) may not be applicable in other applications.

A more general approach is the kinetic Vlasov equation with respect to the distribution function [7], supplemented by a system of Maxwell's equations for electromagnetic fields. This model leads to a partial differential equation of the first order; it is a mathematical formulation of the well-known Liouville theorem on the conservation of phase volume [8]. The properties of the medium, such as particle concentration, charge density, average velocity, etc. are moments of the distribution function.

For the numerical solution of the kinetic equation, methods such as Particle-in-Cell (PiC) and Cloud-in-Cell (CiC) [9] are used. In these methods, the medium is replaced by a set of a finite number of particles possessing macrocharge that interact with each other. Each particle is attributed to the characteristics of the medium: charge, mass, momentum, energy, etc. The average values of these quantities are calculated as the sum of all model particles located in the considered region.

Macroparticles have a finite size, within which the spatial distribution of charge, mass, etc. is set. Most often, this distribution is chosen piecewise constant. In this case, the geometric dimensions of all particles are considered the same. In some works, more complex form-factors of the particles are considered.

The motion of macroparticles obeys the equations of Newtonian mechanics (or relativistic Lorentz equations). This leads to a system of ordinary differential equations (ODEs) for the coordinates and velocities of particles and a system of the Maxwell's equations for electromagnetic fields. For this system, the «leap-frog» scheme is traditionally used. First, electromagnetic fields are set and the change in the coordinates and velocities of the macroparticles is calculated in one time step. Then, according to the changed coordinates

and velocities, the electromagnetic fields are refined. After that, coordinates and velocities are calculated at the next time step, etc.

Based on this approach, Tarakanov developed the KARAT [10] code, which was widely applied to solving various problems of plasma physics. Among them are formation of a virtual cathode, formation of an electron beam in a coaxial diode with magnetic isolation, dynamics of a laser target and the initiation of deuterium-deuterium reactions, focusing of an electron beam and the development of hose instability, anisotropic Waibel instability and many others. We also note the works of Borodachev (see [11] and other works of this author). He proposed several improvements to this approach and performed calculations of a large number of tasks.

The main difficulty of the particle (cloud) method in a cell is the need to introduce space-time discretization separately for particles and separately for electromagnetic fields. This leads to a number of numerical artifacts. Among them are the stroboscopic effect (the onslaught of the phase of the electromagnetic field when its frequency does not match with the sampling frequency in time), non-conservativeness (either the momentum conservation law or the energy conservation law is fulfilled, but not simultaneously), the grid dispersion of the medium, the parasitic increase of shot and grid noise, and some others. This limits the accuracy of this method.

**In the present work,** a new method for calculating the emission problem of a coaxial diode with magnetic isolation is proposed. Instead of particles of finite size, it uses point macroparticles. Their motion is described by relativistic Lorentz equations. The electromagnetic field of the beam is calculated in a static approximation based on the instantaneous position of the particles: the electrostatic field is taken according to the Coulomb law and the magnetic field is according to the Biot–Savart–Laplace law. Edge effects at the cathode boundary are considered insignificant. Test emission calculations are performed and the beam velocity and current are compared with the well-known Fedosov's law. This comparison shows excellent accuracy of the proposed method: the discrepancy between the calculation and the specified theoretical law is no more than 1%. Such accuracy is obviously sufficient for applied calculations.

## 2. Problem statement

Consider the problem of infinite electron emission in the model of a coaxial diode with magnetic isolation (CDMI) in a strong magnetic field [12]. A solid cylindrical conductive cathode with a radius of $R_C$ with a negative potential of $-U$ is located in a cylindrical conductor-anode with a radius of $R_A$ with zero potential in a strong longitudinal magnetic field (figure 1). The entire surface of the cathode, lateral cylindrical and end plane, has the property of infinite emission. As a result, a thin tubular electron beam with a radius of $R_B \approx R_C$ should be formed.

The parameters of the problem are: magnetic field $B = 1$ T $= 10^4$ Gs, diode length $L = 30$ cm, cathode radius $R_C = 1$ cm, anode radius $R_A = 2.72$ cm, cathode potential $U = 511$ kV $= 1.70 \cdot 10^3$ CGS.

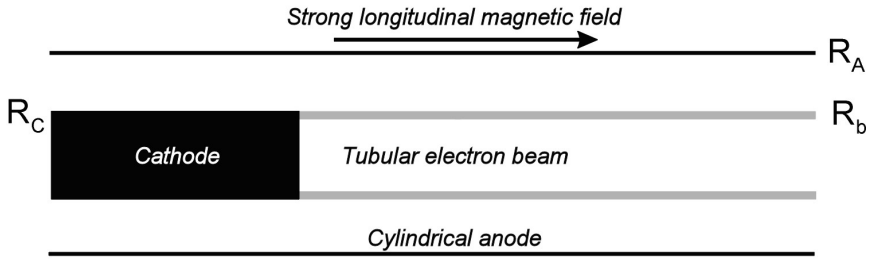


Figure 1. Scheme of the coaxial diode with magnetic isolation

For the current $I$ of a steady beam, the Fedosov's empirical law is valid (see [13] and the cited literature)

$$\begin{gathered} I\ [\mathrm{kA}] = \frac{17.02}{\ln(R_A/R_C)} \frac{\gamma - \gamma_b}{\gamma_b} \sqrt{\gamma_b^2 - 1}, \\ \gamma = 1 + \frac{U\ [\mathrm{kV}]}{511}, \quad \gamma_b = \sqrt{1/4 + 2\gamma} - 1/2. \end{gathered} \tag{1}$$

A theoretical estimate of the $z$-components of the electron beam velocity is also known

$$v_z = c\sqrt{1 - 1/\gamma_b^2}. \tag{2}$$

Here $c$ is the speed of light in vacuum. With the specified task parameters, we have $I \approx 2.7$ kA, $v_z \approx 2.3 \cdot 10^{10}$ cm/s.

## 3. The method of point macroparticles

### 3.1. Point macroparticles

Let the axis $z$ of the coordinate system be directed along the magnetic field and the origin $x = y = z = 0$ correspond to the center of the cathode end face.

On the end surface of the cathode, we select $J$ points $M^j = (x_0^j, y_0^j)$, evenly distributed over this surface. At the initial moment of time, macroparticles containing $Z^j$ electrons fly out of all points. Their initial velocities are supposed to equal zero (i.e., the emission is cold). The emission at a given point of the cathode should be the stronger, the greater the magnitude of the cathode-anode field at this point. Therefore, we choose the value of $Z^j$ proportional to the value of $z$-components of the cathode-anode field at the point $M^j$, i.e.,

$$Z^j = JZ^0 \frac{E_z(M^j)}{\sum\limits_j E_z(M^j)}. \tag{3}$$

Here $Z^0$ is the average charge of one particle. Since in practice $Z_0 \gg 1$, such a particle can be called a macroparticle.

Macroparticles are considered point-size (i.e., the interaction of electrons with each other inside one particle is not taken into account). Macroparticles interact with each other and with external electric and magnetic fields.

Further, at the moment of time $t = \tau$, the second portion of macroparticles flies out of all points $M^j$. For them, the electrostatic field of the first portion of macroparticles partially shields the cathode-anode field. If by the time $t = \tau$ the particles from the first portion do not have time to gain more speed, then they are located relatively close to the end of the cathode, and the shielding turns out to be stronger. Then, at the corresponding points $M^j$, the emission of particles of the second portion weakens. This can be taken into account by reducing the value of $Z^j$ for the second portion. Conversely, if by the time of the second emission, the particles of the first portion managed to gain more speed, then the shielding turns out to be weaker. Then, at the corresponding points $M^j$, the highest charge is emitted, and the value of $Z^j$ for these points must be increased.

The particle movement obeys relativistic equations of motion which are written in terms of momentum, not velocity. Therefore, it is convenient to use the following rule for calculating new $Z^j$

$$Z^j = JZ^0 \frac{p_z^j}{\sum\limits_j p_z^j}. \tag{4}$$

### 3.2. System of equations

Let us write down the equations of motion of the $j$-th macroparticle. We choose momentum and radius vector as unknowns

$$\frac{d\mathbf{r}^j}{dt} = \frac{\mathbf{p}^j}{\sqrt{(p^j)^2/c^2 + (m^j)^2}}, \quad m^j = Z^j m, \tag{5}$$

$$\frac{d\mathbf{p}^j}{dt} = e^j\mathbf{E} + \frac{e^j}{c}\frac{[\mathbf{p}^j \times \mathbf{B}]}{\sqrt{(p^j)^2/c^2 + (m^j)^2}}, \quad e^j = Z^j e. \tag{6}$$

Here $m$, $e$ are the mass and charge of the electron, $\mathbf{E}$, $\mathbf{B}$ are the total electric and magnetic fields in which the $j$-th particle moves.

Electric field $\mathbf{E} = \mathbf{E}^{\text{ext}} + \mathbf{E}^{el}$ is the sum of the external cathode-anode field $\mathbf{E}^{\text{ext}}$ and the electrostatic field $\mathbf{E}^{el}$ created by other electrons. According to the Coulomb law, we have

$$\mathbf{E}^{el} = \sum_{i \neq j,\, Z^i \neq 0} e^j \frac{\mathbf{r}^j - \mathbf{r}^i}{|\mathbf{r}^j - \mathbf{r}^i|^3}. \tag{7}$$

The sum is taken for all particles that have flown out of the cathode at a given time.

Magnetic field $\mathbf{B} = \mathbf{B}^{\text{ext}} + \mathbf{B}^{el}$ consists of an external solenoid field $\mathbf{B}^{\text{ext}}$ and a field $\mathbf{B}^{el}$, which is created by other electrons when moving. The field $\mathbf{B}^{el}$ is described by the Biot–Savart–Laplace law

$$\mathbf{B}^{el} = \sum_{i \neq j,\, Z^i \neq 0} \frac{e^j}{c} \frac{[\mathbf{v}^i, \mathbf{r}^j - \mathbf{r}^i]}{|\mathbf{r}^j - \mathbf{r}^i|^3}. \tag{8}$$

### 3.3. Numerical method

The equations of motion are solved numerically according to the explicit Runge–Kutta scheme of the 4th order of accuracy. To increase the mathematical accuracy of the difference scheme, the time interval $\tau$ can be divided into several steps, during which the number of particles does not change.

The potential of the cathode-anode field is found by solving the boundary value problem for the Laplace equation. It is considered in a cylindrically symmetric formulation. On the walls of the anode, the potential is assumed to be zero, and on the cathode — equal to $-U$. The solution uses the package FreeFem++[14]. Figure 2 shows potential isolines and field strength vectors in coordinates $z - \rho$, where $\rho = \sqrt{x^2 + y^2}$ is the polar radius. For clarity, the range of variation of $z$ is limited to the value of $z = 5$. Note that this cathode-anode field decreases rapidly as $z$ increases. The maximum voltage is reached near the cathode rib.

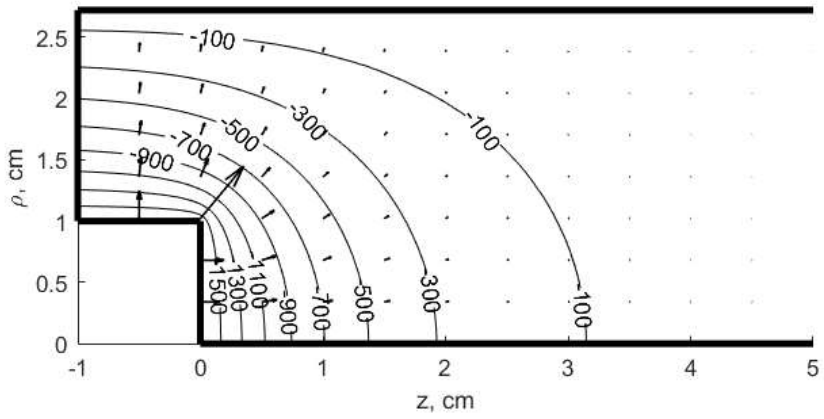


Figure 2. The potential and the cathode-anode field strength in units of CGS. Solid line is the boundary of the computational domain

### 3.4. Remarks

**1)** The fundamental difference between the proposed approach and the traditional PiC/CiC method is that macroparticles are considered point-like. This makes it possible to write out explicit expressions for the electric and magnetic fields created by particles. Therefore, during the calculation, it is not necessary to solve the system of the Maxwell's equations. This not only gives a gain in efficiency, but also eliminates the previously mentioned numerical artifacts that arise in the traditional particle method. This is an advantage of the point macroparticle method.

**2)** Quasi-static expressions for the fields (7) and (8) are approximate. They do not take into account the boundary effects at the anode boundaries.

The interaction of charges with walls can be taken into account by the method of electro- and magnetostatic images [15]. A separate issue is the accuracy with which the timebase of the fields (7) and (8) satisfy the Maxwell's equations. Related to the period of the REB formation, this issue requires additional research and is beyond the scope of this work. After the REB is formed and can be considered steady, temporal dependence of the field vanishes (at least, in some vicinity of the cathode). In this case, fulfillment of the Maxwell's equations is provided by employment of the Coulomb and the Biot–Savart–Laplace laws.

## 4. Calculation results

Let us take $J = 3000$, $\tau = 10^{-11}$ s. Then $Z^0 = 5.956 \cdot 10^7$. The location of the points $M^j$ at the end of the cathode corresponds to figure 3 (far left).

The calculation was carried out up to the time $t = 10^{-9}$ s, i.e., at the end of the calculation, the number of macroparticles reached $\sim 3 \cdot 10^5$. At the same time, the particles of the first portion reached the section $z \approx 28$, the steady beam corresponds to the segment $0 \leqslant z \leqslant 8$.

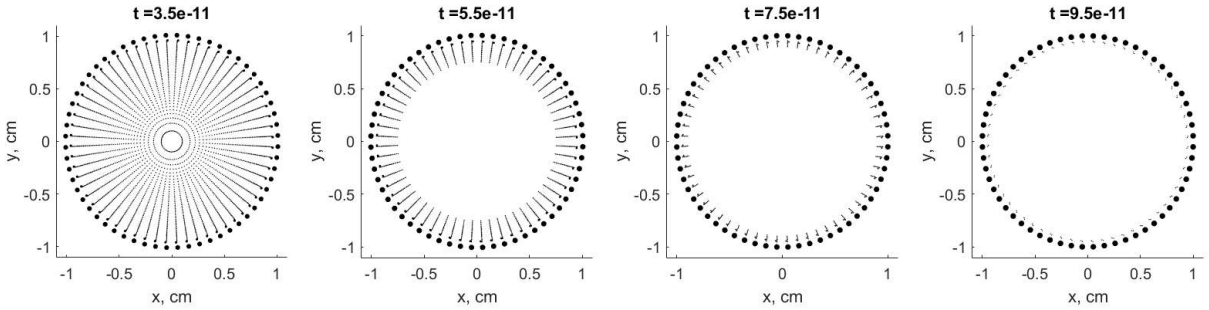


Figure 3. Cross sections of the beam with a plane $z = 0$ at time moments $t = 0.035, 0.055, 0.075, 0.095$ ns (from left to right)

Figure 3 shows the cross sections of the beam with the plane $z = 0$ at several consecutive moments of time. These moments are indicated above the graphs. The points are the intersection of the trajectories of the macroparticles with the specified plane. The size of the markers is proportional to the charge of the macroparticles. Particles with a charge less than $10^{-3}Z^0$ are not displayed.

It can be seen that at the initial moment of time, emission occurs from the entire surface of the cathode end face. Over time, the emission is suppressed first in the center of the cathode, and a tubular beam begins to form. Then the area in which the emission is suppressed expands, and the tube wall becomes thinner. Finally, a thin-walled beam is installed.

In figure 4, the dependence of the average $z$ component of the electron velocity in a steady beam on the $z$ coordinate is presented. It can be seen that with an increase in $z$, the value of $v_z$ increases rapidly and at $z \approx 3$ cm goes to a constant value of $v_z = 2.30 \cdot 10^{10}$ cm/s. This value perfectly agrees with the theoretical value obtained from the Fedosov's law: the difference is only 0.01%.

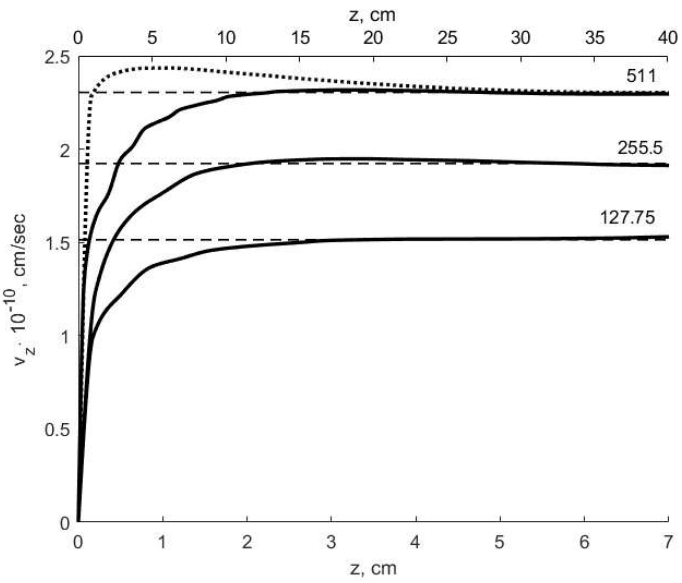


Figure 4. Average component $v_z$ of the electron velocity. Solid line is calculation for $R_A/R_C = 2.72$, dotted line is calculation for $R_A/R_C = 5.44$ (upper axis of abscissa), dashed line is theoretical estimate from the Fedosov's law. The numbers near the lines are the value of the cathode-anode potential $U$

Figure 5 shows the dependence of the beam current $I$ on the coordinate $z$. It is clearly seen that with the growth of $z$, the current value increases rapidly and reaches a constant value of $I = 2.86$ kA, which perfectly agrees with the Fedosov' law. The deviation of the right end of the curve from the horizontal is due to the fact that the beam is not fully established.

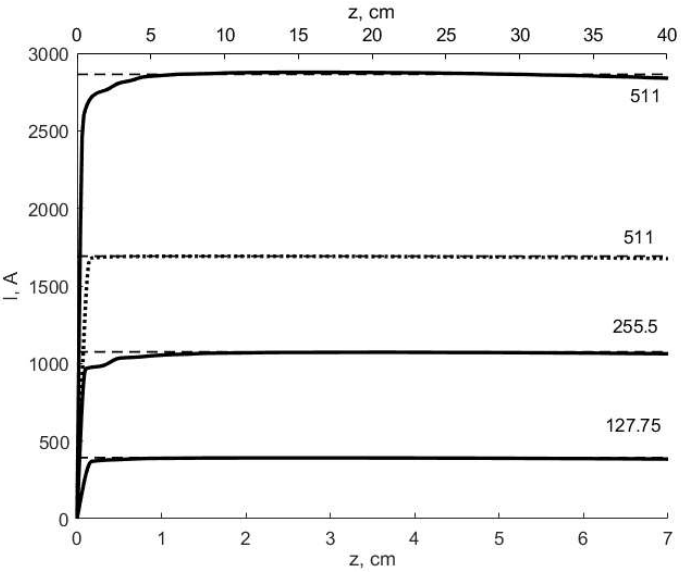


Figure 5. Beam current. Solid line is calculation for $R_A/R_C = 2.72$, dotted line is calculation for $R_A/R_C = 5.44$ (upper axis of abscissa), dashed line is theoretical estimate from the Fedosov' law. The numbers near the lines are the value of the cathode-anode potential $U$

# 5. Parameter selection

In this section, we show that the velocity and current of the steady-state beam practically do not depend on the values of the user-defined parameters $J$ and $\tau$.

## 5.1. Number of particles

Let us perform the calculation with $J = 120$, $\tau = 10^{-11}$ s. Then $Z^0 = 1.489 \cdot 10^9$. This value is 25 times different from the one specified in section 4. Figure 6 shows a comparison of the profiles of the average $z$-velocity components depending on $z$ for calculations with $J = 3000$ and $J = 120$. It can be seen that the qualitative behavior of both curves coincides. The initial sections corresponding to a sharp increase in $v_z$ are somewhat different. But at $z \geqslant 2$, both curves come out to the same constant value that coincides with the theoretical value (2). The calculated velocities of the steady-state beam are consistent with the theoretical estimate with an accuracy better than 0.5%.

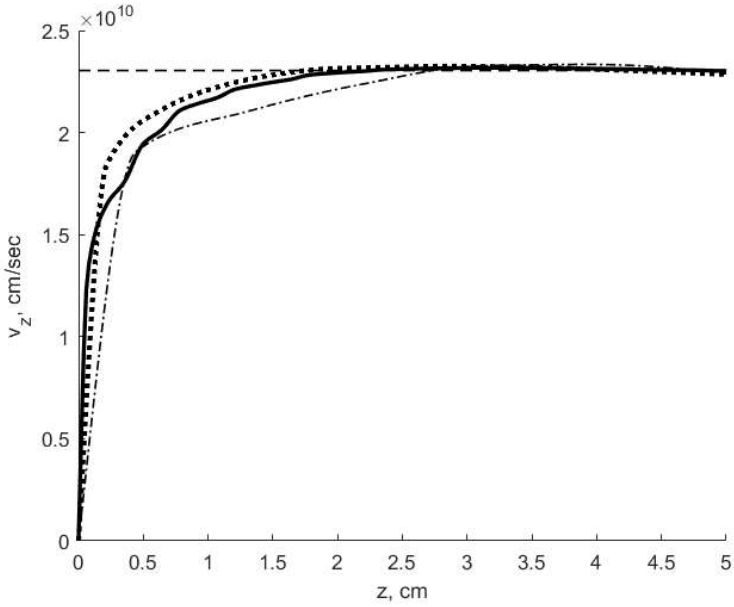


Figure 6. The average $z$ speed component for $U = 511$ kV, $R_A/R_C = 2.72$. Solid line is calculation with $J = 3000$, $\tau = 10^{-11}$ s, dotted line is calculation with $J = 120$, $\tau = 10^{-11}$ s, dashed line is calculation with $J = 120$, $\tau = 2 \cdot 10^{-11}$ s, dashed line is theoretical estimate from the Fedosov's law

In figure 7, a similar comparison of beam current profiles for calculations with $J = 3000$ and $J = 120$ is presented. It can be seen that both curves practically coincide and quickly tend to the theoretical value determined by the Fedosov's law (1). The calculated values of the steady-state beam current are consistent with the theoretical estimate with an accuracy better than 0.3%.

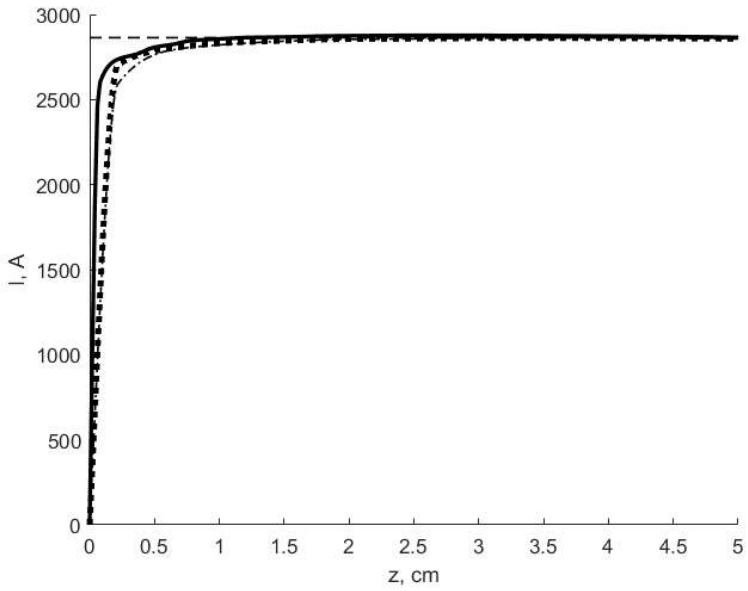


Figure 7. Beam current for $U_0 = 511$ kV, $R_A/R_C = 2.72$. The designations correspond to figure 6

### 5.2. Time interval between particle portions

Let us perform the calculation with $J = 120$, $\tau = 2 \cdot 10^{-11}$ s. To increase the mathematical accuracy, we divide the interval $\tau$ into 2 intermediate steps of the difference scheme. In this calculation, $Z^0 = 2.978 \cdot 10^9$. This value differs by 2 times from the one specified in 5.1. Figure 6 shows a comparison of $v_z$ profiles depending on $z$ for calculations with $\tau = 10^{-11}$ s and $\tau = 2 \cdot 10^{-11}$ s. It can be seen that both curves increase rapidly and tend to constant values that coincide with the theoretical estimate (2). The agreement with the theoretical estimate turns out to be better than 1%.

Figure 7 shows a similar comparison of beam current profiles for calculations with $\tau = 10^{-11}$ s and $\tau = 2 \cdot 10^{-11}$ s. It can be seen that both curves practically coincide and quickly reach the theoretical value of the current determined by the Fedosov's law. The accuracy with which the calculation is consistent with the theoretical estimate turns out to be better than 0.5%.

## 6. Verification of the model

### 6.1. Cathode-anode potential

To test the model, we will perform similar calculations for other values of the cathode-anode potential $U = 511/2 = 255.5$ kV and $U = 511/4 = 127.75$ kV. In both calculations, we put $J = 120$, $\tau = 10^{-11}$ s. The dependence of the $z$-components of the electron velocity on the $z$ coordinate for both calculations is shown in figure 4. It can be seen that with an increase in $z$, the value of $v_z$ increases from zero to $1.95 \cdot 10^{10}$ cm/s in the first calculation and to $1.52 \cdot 10^{10}$ cm/s in the second calculation. The obtained velocities are in

excellent agreement with the theoretical values: the difference does not exceed 0.3%.

Figure 5 shows the dependence of the beam current on the $z$ coordinate in both calculations. It can be seen that with the growth of $z$, the current value increases rapidly and reaches a constant value of $I = 1.07$ kA for $U = 255.5$ kV and $I = 0.39$ kA for $U = 127.75$ kV. From figure 5, it can be seen that these values perfectly agree with the Fedosov current: in both calculations, the discrepancy does not exceed 0.5%.

### 6.2. Ratio of cathode and anode radii

Let us make calculations for a different ratio of the radii of the anode and cathode $R_A/R_C = 2.72 \cdot 2 = 5.44$. We take $J = 120$, $\tau = 10^{-11}$ s. The dependence of the average $z$-velocity component on the $z$ coordinate is shown in figure 4. Since the beam is established at a significantly greater distance from the cathode than in the calculations of 4, a separate abscissa axis was used. It can be seen that with an increase in $z$, the value of $v_z$ increases, passes through the maximum, then decreases and tends to a constant value. The latter perfectly agrees with the estimate from the Fedosov's law: the discrepancy does not exceed 0.5%.

Figure 5 shows the dependence of the beam current on the $z$ coordinate (the upper axis of the abscissa). It can be seen that the current quickly tends to a constant value that coincides with the Fedosov current with an accuracy not worse than 0.6%.

## 7. Conclusion

The proposed algorithm provides self-consistent emission suppression in the center of the cathode and the formation of a tubular electron beam. The dependence of the average $z$ component of the macroparticles velocity and the beam current on $z$ reproduces the known quantitative regularities with good accuracy. This confirms the correctness of the calculation results. It is shown that the calculated particle velocity and current in a steady beam do not depend on the parameters set by the user.

## Acknowledgments

This work was supported by grant MK-3630.2021.1.1.

## References

[1] M. V. Kuzelev *et al.*, "Plasma relativistic microwave electronics," *Plasma Physics Reports*, vol. 27, no. 8, pp. 669–691, 2001. DOI: 10.1134/1.1390539.

[2] S. P. Bugaev, E. A. Litvinov, G. A. Mesyats, and D. I. Proskurovskii, "Explosive emission of electrons," *Physics Uspekhi*, vol. 18, no. 1, pp. 51–61, 1975. DOI: 10.3367/UFNr.0115.197501d.0101.

[3] O. T. Loza and I. E. Ivanov, "Measurements of the transverse electron velocities in high-current microsecond relativistic electron beams in a strong magnetic field," *Technical Physics*, vol. 48, no. 9, pp. 1180–1185, 2003. DOI: 10.1134/1.1611905.

[4] D. K. Ul'yanov *et al.*, "Controlling the radiation frequency of a plasma relativistic microwave oscillator during a nanosecond pulse," *Technical Physics*, vol. 58, no. 10, pp. 1503–1506, 2013. DOI: 10.1134/S1063784213100265.

[5] S. Y. Belomyttsev, A. A. Grishkov, S. D. Korovin, and V. V. Ryzhov, "The current of an annular electron beam with virtual cathode in a drift tube," *Technical Physics Letters*, vol. 29, no. 7, pp. 666–668, 2003. DOI: 10.1134/1.1606783.

[6] S. V. Polyakov, "Mathematical modeling using multiprocessor computing systems of electronic transport processes in vacuum and solid-state micro- and nanostructures [Matematicheskoye modelirovaniye s pomoshch'yu nogoprotsessornykh vychislitel'nykh sistem protsessov elektronnogo transporta v vakuumnykh i tverdotel'nykh mikro- i nanostrukturakh]," in Russian, Diss. ... Doctor of Physical and Mathematical Sciences, M. V. Keldysh IAM, RAS, 2010.

[7] A. A. Vlasov, "The vibrational properties of an electron gas," *Physics Uspekhi*, vol. 10, no. 6, pp. 721–733, 1968. DOI: 10.3367/UFNr.0093.196711f.0444.

[8] I. A. Kvasnikov, *Thermodynamics and statistical physics. Vol. 3. Theory of nonequilibrium systems [Termodinamika i statisticheskaya fizika, Tom 3, Teoriya ravnovesnykh sistem, Teoriya neravnovesnykh sistem]*. Moscow: URSS, 2003, in Russian.

[9] R. W. Hockney and J. W. Eastwood, *Computer simulation using particles*. McGraw-Hill Inc., 1981.

[10] V. P. Tarakanov, *User's Manual for Code KARAT*. Va, USA: BRA Inc., 1992.

[11] L. V. Borodachev, "Discrete modeling of low-frequency processes in plasma [Diskretnoye modelirovaniye nizkochastotnykh protsessov v plazme]," in Russian, Diss. ... Doctor of Physical and Mathematical Sciences, M. V. Lomonosov MSU, 2012.

[12] V. V. Andreev *et al.*, *Physical electronics and its modern applications [Fizicheskaya elektronika i yeye sovremennyye prilozheniya]*. Moscow: RUDN University, 2008, in Russian.

[13] S. E. Ernyleva, V. O. Litvin, O. T. Loza, and I. L. Bogdankevich, "Promising source of high-power broadband microwave pulses with radiation frequency variable up to two octaves," *Technical Physics*, vol. 59, no. 8, pp. 1228–1232, 2014. DOI: 10.1134/S1063784214080106.

[14] F. Hecht, "New development in FreeFem++," *Journal of numerical mathematics*, vol. 20, no. 3–4, pp. 251–266, 2012. DOI: 10.1515/jnum-2012-0013.

[15] V. I. Denisov, *Introduction to electrodynamics of material media [Vvedeniye v elektrodinamiku material'nykh sred]*. Moscow: M. V. Lomonosov MSU, 1989, in Russian.

**For citation:**
A. A. Belov, O. T. Loza, K. P. Lovetskiy, S. P. Karnilovich, L. A. Sevastianov, Numerical simulation of cold emission in coaxial diode with magnetic isolation, Discrete and Continuous Models and Applied Computational Science 30 (3) (2022) 217–230. DOI: 10.22363/2658-4670-2022-30-3-217-230.

**Information about the authors**:

**Belov, Aleksandr A.** — Candidate of Physical and Mathematical Sciences, Researcher of Faculty of Physics, M. V. Lomonosov Moscow State University; Assistant professor of Department of Applied Probability and Informatics of Peoples' Friendship University of Russia (RUDN University) (e-mail: aa.belov@physics.msu.ru, phone: +7(495)9393310, ORCID: https://orcid.org/0000-0002-0918-9263, ResearcherID: Q-5064-2016, Scopus Author ID: 57191950560)

**Loza, Oleg T.** — Doctor of Physical and Mathematical Sciences, Professor of Institute of Physical Research and Technology of Peoples' Friendship University of Russia (RUDN University) (e-mail: loza-ot@rudn.ru, phone: +7(495)9550822, ORCID: https://orcid.org/0000-0003-4676-6303)

**Lovetskiy, Konstantin P.** — Candidate of Physical and Mathematical Sciences, Associate professor of Department of Applied Probability and Informatics of Peoples' Friendship University of Russia (RUDN University) (e-mail: lovetskiy-kp@rudn.ru, phone: +7(495)9522572, ORCID: https://orcid.org/0000-0002-3645-1060)

**Karnilovich, Sergey P.** — Candidate of Physical and Mathematical Sciences, Assistant professor of Institute of Physical Research and Technology of Peoples' Friendship University of Russia (RUDN University) (e-mail: karnilovich-sp@rudn.ru, phone: +7(495)4344212, ORCID: https://orcid.org/0000-0001-5696-1546)

**Sevastianov, Leonid A.** — Doctor of Physical and Mathematical Sciences, Professor of Department of Applied Probability and Informatics of Peoples' Friendship University of Russia (RUDN University) (e-mail: sevastianov-la@rudn.ru, phone: +7(495)9522572, ORCID: https://orcid.org/0000-0002-1856-4643)

УДК 519.872:519.217
PACS 07.05.Tp, 02.60.Pn, 02.70.Bf
DOI: 10.22363/2658-4670-2022-30-3-217-230

# Численное моделирование холодной эмиссии в коаксиальном диоде с магнитной изоляцией

**А. А. Белов[1, 2], О. Т. Лоза[2], К. П. Ловецкий[2], С. П. Карнилович[2], Л. А. Севастьянов[2]**

[1] *Московский государственный университет им. М. В. Ломоносова, Ленинские горы, д. 1, стр. 2, Москва, 119991, Россия*
[2] *Российский университет дружбы народов, ул. Миклухо-Маклая, д. 6, Москва, 117198, Россия*

**Аннотация.** В связи с появлением и активным развитием новых областей применения мощных и сверхмощных электровакуумных приборов СВЧ возрос интерес к изучению особенностей поведения ансамблей заряженных частиц, движущихся в пространстве взаимодействия. Примером является пучок электронов, формируемый в коаксиальном диоде с магнитной изоляцией. Численное моделирование эмиссии в таком диоде традиционно проводится с помощью методов типа «частица в ячейке». Они основаны на одновременном расчете уравнений движения частиц и уравнений Максвелла для электромагнитного поля. В данной работе предложен новый вычислительный подход, названный методом точечных макрочастиц. В нем движение частиц описывается уравнениями релятивистской механики, а для полей выписываются явные выражения в квазистатическом приближении. Выполнены расчеты формирования релятивистского электронного пучка в коаксиальном диоде с магнитной изоляцией и проведено сравнение с известными теоретическими соотношениями для скорости электронов в пучке и для тока пучка. Получено отличное согласование результатов расчета с теоретическими формулами.

**Ключевые слова:** коаксиальный диод с магнитной изоляцией, холодная эмиссия, точечные макрочастицы